Consequences of Counterion Mutation in Sensory Rhodopsin II of *Natronobacterium pharaonis* for Photoreaction and Receptor Activation: An FTIR Study†

Michael Hein,‡ Ionela Radu,‡ Johann P. Klare,§ Martin Engelhard,§ and Friedrich Siebert*,‡

Sektion Biophysik, Institut für Molekulare Medizin und Zellforschung, Albert-Ludwigs-Universität, Hermann-Herderstrasse 9, 79104 Freiburg, Germany, and Max-Planck-Institut für Molekulare Physiologie, Otto-Hahnstrasse 11, 44227 Dortmund, Germany

Received August 12, 2003; Revised Manuscript Received November 27, 2003

ABSTRACT: In many retinal proteins the proton transfer from the Schiff base to the counterion represents a functionally important step of the photoreaction. In the signaling state of sensory rhodopsin II from *Natronobacterium pharaonis* this transfer has already occurred, but in the counterion mutant Asp75Asn it is blocked during all steps of the photocycle. Therefore, the study of the molecular changes during the photoreaction of this mutant should provide a deeper understanding of the activation mechanism, and for this, we have applied time-resolved step-scan FTIR spectroscopy. The photoreaction is drastically altered; only red-shifted intermediates are formed with a chromophore strongly twisted around the 14−15 single bond. In addition, the photocycle is shortened by 2 orders of magnitude. Nevertheless, a transition involving only protein changes similar to that of the wild type is observed, which has been correlated with the formation of the signaling state. However, whereas in the wild type this transition occurs in the millisecond range, it is shortened to 200 μs in the mutant. The results are discussed with respect to the altered electrostatic interactions, role of proton transfer, the published 3D structure, and physiological activity.

Sensory rhodopsin II from *Natronobacterium pharaonis* (NpSRII)[1] enables the cell to avoid conditions of high oxygen concentrations in the presence of intensive light (*1*). This pigment, which was originally named phoborhodospin (*2*), is closely related to sensory rhodopsin I, another phototaxis receptor, and the two light-activated ion pumps halorhodopsin and bacteriorhodopsin (BR) (reviewed in refs *3* and *4*). The structure of NpSRII has recently been determined, which is strikingly similar to that of BR (*5*, *6*). Major differences concern the extracellular channel in which the guanidinium group of Arg72 points away from the retinylidene Schiff base. Additionally, the cytoplasmatic channel is blocked because Asp96 in BR is replaced by phenylalanine (Phe76). The photocycle of NpSRII displays the canonical intermediates of the BR photocycle, although the absorption maxima are blue shifted (*7*, *8*). The turnover of the NpSRII photocycle is almost 2 orders of magnitude slower than that of BR, an observation that is responsible for the poor proton pumping efficiency (*9*). A mutational study in which key residues important for the efficient proton transfer in BR were introduced into NpSRII did not succeed in obtaining the kinetic properties of BR (*10*).

From the channel mutations, that at position 75 is of special interest. The abolition of the carboxyl function at the position of the counterion will support the assignment of a band observed with the formation of the M intermediate at 1764 cm^{-1} (*11*, *12*) to the C═O stretching mode of this residue, demonstrating that it becomes protonated with Schiff base deprotonation. On the basis of a downshift observed in the Asp75Glu mutant, this band has been assigned previously to protonation of the counterion (*13*). In visual pigments the neutralization of the negative charge at the counterion position is thought to represent a key step in receptor activation (*14*), and it has been shown that it causes constitutive activity, i.e., receptor activation without the presence of the chromophore and, therefore, without the action of light. Binding of the native 11-*cis*-retinal chromophore re-forms the dark state and turns this activity off. A related observation has been made for sensory rhodopsin II from *Halobacterium salinarum* (HsSRII): here, constitutive activity has been observed by neutralization of the negative charge at the counterion position 73 even in the presence of the chromophore. This activity is increased by the action of light, although it does not reach the level of the wild-type receptor (*15*). From this, a general model for the mechanism of retinal protein photoreceptors and ion pumps has been developed (*16*). The role of the salt bridge formed by the negative counterion and the positive protonated Schiff base in the early steps of the photoreaction of retinal proteins has been addressed in theoretical calculations (*17*, *18*). In bacteriorhodopsin, in which the negative charge of the counterion Asp85 has been neutralized by protonation,

† Work supported by the Deutsche Forschungsgemeinschaft, Grants SI 278/18-3,4 (to F.S.) and EN 87/10-3,4 (to M.E.), and by Fonds der Chemischen Industrie (to F.S.).

* To whom correspondence should be addressed. E-mail: frisi@biophysik.uni-freiburg.de. Phone: (49) 761 203 5396. Fax: (49) 761 203 5399.

‡ Albert-Ludwigs-Universität.

§ Max-Planck-Institut für Molekulare Physiologie.

[1] Abbreviations: FTIR, Fourier transform infrared; HOOP, hydrogen out of plane; NpSRII, sensory rhodopsin II from *N. pharaonis*.

10.1021/bi0354381 CCC: $27.50
Published on Web 12/31/2003

an intermediate very similar to the L state has been identified by FTIR spectroscopy (*19*). This indicates a minor role of this salt bridge for the early part of the photocycle (corresponding investigations of the Asp85Asn mutant are complicated by the presence of several dark states being in an pH- and anion-dependent equilibrium, and no IR or resonance Raman studies of the early intermediates have been published). On the other hand, time-resolved UV−vis studies on the early step of the photoreaction indicated a kinetic role, neutralization slowing down photoisomerization (*20*).

The Asp75Asn mutant of NpSRII has been investigated by time-resolved UV−vis spectroscopy and by electrical measurements (*9*). The most striking observation is a considerable shortening of the photocycle. A transient electrical signal has been described which is directed oppositely to the proton pumping direction of bacteriorhodopsin, and a similar signal has been described for the red-shifted species of the corresponding mutant of bacteriorhodopsin, Asp85Asn (*21*). Since no state corresponding to M has been detected, the molecular origin of these signals cannot be correlated with proton transfer steps. Probably, they reflect movements of the positively charged Schiff base or other charged or polar groups, induced by the chromophore isomerization. The molecular changes occurring with the formation of the K intermediates of wild-type NpSRII and the Asp75Asn mutant have also been studied by photoacoustic measurements. The volume changes are comparable in these two systems, and they are considerably larger than those of bacteriorhodopsin (*22*, *23*). This indicates that the global molecular alterations are not strongly affected by the mutation.

Previously, we have studied the molecular changes of NpSRII evolving during the photocycle by time-resolved FTIR spectroscopy (*12*). As compared to bacteriorhodopsin, the K intermediate of NpSRII was characterized by larger amide I bands, indicating larger changes of the protein backbone. Only small additional changes take place with the formation of L. In M, the Schiff base is deprotonated, and a carboxyl group becomes protonated. In view of the similar observation in bacteriorhodopsin, and since in the Asp75Asn mutant no M is formed, this group has been tentatively identified with the counterion Asp75, which has been confirmed independently (*13*). Importantly, within the lifetime of the M state a transition has been observed only involving changes of the protein. Using the spin label technique, this step has been identified with the outward tilting of helix F (H.-J. Steinhoff and M. Engelhard, unpublished observation) that has been described before (*24*). Finally, the chromophore geometry in the O state has been determined to be all-trans. Together with measurements performed in the presence of azide which causes a fast reprotonation of the Schiff base, this shows that neither Schiff base reprotonation nor the thermal reisomerization of the chromophore is the rate-limiting step for the photocycle duration and that the long cycling time must be an inherent property of the protein which guarantees that enough time is allowed for the signaling state to transfer the information to the later steps of the signal transduction cascade.

In this paper we describe static low-temperature and time-resolved step-scan FTIR investigations on the photoreaction of the Asp75Asn mutant of NpSRII. We confirm the observations that the photocycle of the mutant is considerably shortened and that only red-shifted intermediates are observed. Although no M state is formed, a transition reflecting only protein structural changes also takes place in this mutant, and the amide spectral changes are very similar to those of the corresponding transition of the wild-type protein. The results are discussed with respect to the reported activation properties of this receptor mutant. In addition, we discuss some aspects of the color tuning mechanism in the dark state and K intermediate.

MATERIALS AND METHODS

The expression of NpSRII and its Asp75Asn mutant in *Escherichia coli* and the reconstitution into lipids from *N. pharaonis* were described recently (*9*).

The static UV−vis and FTIR measurements have been performed as described recently for the wild-type protein (*12*). The photoreaction was induced by illumination with light between 450 and 500 nm for 1 min, using a slide projector and attached fiber optics. Approximately 2 nmol of NpSRII reconstituted into lipids from *N. pharaonis* was deposited onto a BaF_2 window, rehydrated, and sealed with a second window. The pH was adjusted to 8 by adding 500 nmol of the appropriate phosphate buffer. For measurements in ^2H_2O, the protein film on the BaF_2 window was dried five times and rehydrated with 5 μL of ^2H_2O, until the final hydration was adjusted. Spectral resolution for the FTIR measurements was 4 cm^{-1}, and usually 512 scans were accumulated for the single beam spectra of both the dark and illuminated states. It is important to mention that the low-temperature photoproduct was completely driven back to the dark state by illumination with red light (>570 nm).

The acquisition of the time-resolved step-scan FTIR spectra has been described recently (*12*, *25*). Excitation was provided by a Nd:YAG laser coupled to an OPO, providing a pulse of 1.5 mJ at 490 nm within 4 ns. The repetition rate was 5 Hz. We used mainly our system with a time resolution of 600 ns; however, a few experiments were obtained with a time resolution of 30 ns (*25*), allowing the comparison of the respective early intermediates. For each step-scan run eight signals were averaged at each sampling position, and the results of eight measurements had been co-added. The spectral resolution was 8 cm^{-1}, and the measuring temperature was 25 °C. The time-resolved difference spectra had been analyzed as described before for the wild-type protein. They were fitted to a sum of exponentials, from which the amplitude spectra were obtained. From the amplitude spectra intermediate spectra were calculated using the unidirectional reaction scheme without back-reactions.

RESULTS

Static Low-Temperature Difference Spectra. We first studied the photoreaction at low temperature by static UV−vis difference spectroscopy. In contrast to the wild-type protein, the yield of photoproduct formation is temperature dependent above 80 K, increasing from 90 to 150 K, subsequently remaining constant up to 165 K. At higher temperatures the photoproduct starts to decay to the initial state. The shape of the corresponding difference spectrum does not differ for the various temperatures, especially the isosbestic point remaining fixed (data not shown). This indicates that only one photointermediate is involved. We

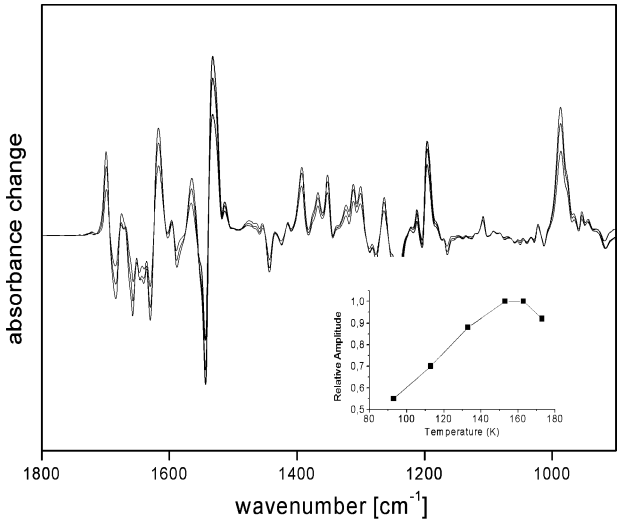

FIGURE 1: Temperature dependence of the photoproduct yield at low temperature. Shown are the spectra obtained at 113, 133, and 153 K with increasing amplitude. The insert shows the dependence over a somewhat wider range, the decrease at 173 K caused by the slow decay of the photoproduct during the data acquisition (1 min).

deduce an approximate absorption maximum around 560 nm, in agreement with time-resolved UV−vis measurements (*9*). This is corroborated by the corresponding infrared difference spectra (Figure 1). They are almost identical to each other, only the size of the bands varies according to the temperature-dependent photoproduct yield and stability. Representative difference spectra obtained in H_2O and ^2H_2O at 113 K are shown in Figure 2b,c, together with a corresponding difference spectrum of the wild type measured in H_2O at 103 K (Figure 2a) (*12*).

Between 1300 and 1100 cm^{-1} the comparison of wild-type and mutant spectra reveals great similarities. The large fingerprint bands in this spectral region show that the common all-trans → 13-cis isomerization has taken place. In other spectral regions, however, considerable deviations are evident. The HOOP mode at 989 cm^{-1} has much higher intensity and is slightly downshifted, whereas the smaller HOOP bands are not altered. This large band is, as the smaller band in the wild-type spectrum, assigned to the C15−HOOP (hydrogen out of plane) mode since it is downshifted to 976 cm^{-1} by Schiff base deuteration (Figure 2c). The larger size indicates that the chromophore is less relaxed and more twisted around the C14−C15 single bond. This must be caused by the altered interaction of the Schiff base with the now neutral environment. The difference band at 1543(−)/1532(+) cm^{-1} has higher intensity than the corresponding band at 1552(−)/1542(+) cm^{-1} in the wild-type spectrum. This shows that there is little overlap of the bands and the positions agree with the corresponding absorption maxima of the dark state (520 nm) and the photoproduct (565 nm) described above (see ref *26*) for the correlation of the absorption maximum and the ethylenic stretching frequency). For the wild-type receptor a much smaller shift from 500 to 511 nm has been identified (*7*, *12*). Previously, we have explained the apparent discrepancy between the small red shift and the rather large band separation of 10 cm^{-1}: if the band shift is considerably smaller than the bandwidth, the band separation in the difference band is essentially given by the bandwidth, a larger shift at first causing a higher intensity (*12*). Below we will propose mechanisms explaining

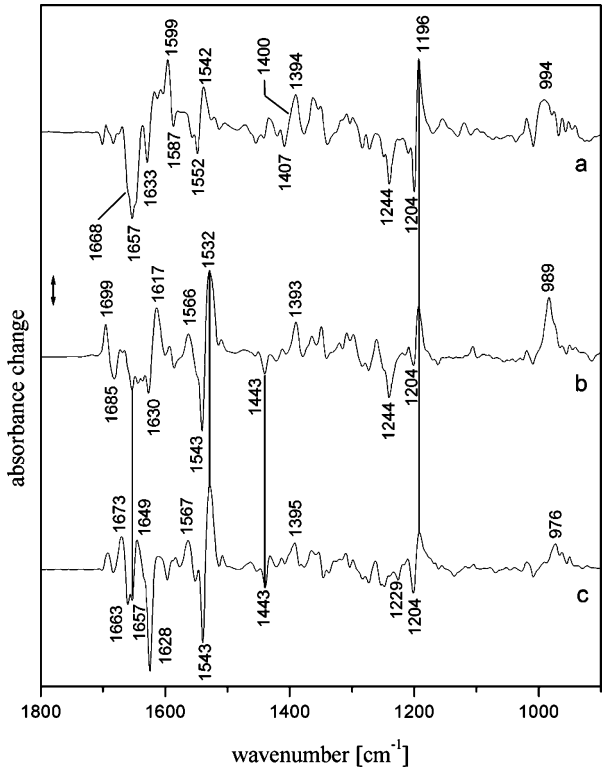

FIGURE 2: Static low-temperature FTIR difference spectra of wild-type NpSRII obtained at 103 K (a) and of the Asp75Asn mutant obtained at 113 K (b). Spectrum c shows the corresponding spectrum of the mutant measured in ^2H_2O. Other measurement conditions are given in Materials and Methods. Spectrum a is from ref *12*). The double arrow corresponds to 1 mOD.

the differences in the spectral shifts of the two proteins. The red shift of the absorption maximum and the characteristic HOOP mode justify to term this intermediate the K state of the Asp75Asn mutant.

Deviations between the two spectra are also evident above 1580 cm^{-1}. The difference band at 1599(−)/1587(+) cm^{-1} is missing, and a new large positive band shows up at 1617 cm^{-1}. In addition, a new pronounced difference band shows up at 1699(+)/1685(−) cm^{-1}. Because of its position and its shift induced by ^2H_2O to 1673(+)/1663(−) cm^{-1}, we assign this last band to the C═O stretch of substituting Asn75. (The remaining small positive band could arise from nonexchanged Asn75 or from a different residue hidden under the 1699/1685 difference band.) A similar downshift has been described for asparagine in ^2H_2O (*27*). Bands at comparable positions have been induced by the Asp96Asn mutation of bacteriorhodopsin (*28*) and of Asp83Asn and Glu122Gln mutations of rhodopsin (*29*). The upshift in K indicates that the C═O group becomes less hydrogen bonded. One explanation could be that the interaction of the positively charged Schiff base with the C═O group of Asn75 is reduced by the isomerization. But also a small reorientation of the Asn75 side chain, changing the interaction of the C═O group, could cause such an upshift. In addition, changes in the interaction of the protein with the NH_2 group of Asn75 can also influence the position, since the C═O stretch is coupled to the $\delta(NH_2)$ vibration.

In the spectral range between 1680 and 1610 cm^{-1} amide I bands and the C═N stretch of the protonated Schiff base contribute. Schiff base deuteration shifts this latter band down, providing a simple means to identify this mode. One

has, however, to consider the possibility that amide I bands can also be shifted in the same direction by a few wavenumbers if hydrogen can be exchanged for deuterium at the involved peptide bonds. The spectrum obtained in ^2H_2O (Figure 2c) shows that the negative band at 1640 cm^{-1} disappears and a new large negative band at 1628 cm^{-1} appears. This large shift is not explainable by amide bands. Therefore, we assign the bands to the C═N stretching modes of the protonated and deuterated Schiff base, respectively, of the mutant dark state. The corresponding values for the wild-type protein at 1657 and 1633 cm^{-1} have been published recently (*30*) and are in agreement with our own measurements (*12*).

Having identified the C═N stretch mode of the dark state, we can now conclude that the mutation also influences the amide I bands. The band corresponding to the shoulder at 1668 cm^{-1} in the wild-type spectrum is missing, and instead, a new negative band at 1657 cm^{-1} appears which, however, is not influenced by deuteration (in contrast to the C═N stretch of the wild type located at the same position). The general size of amide bands is similar in the two spectra, indicating that the extent of distortions of the peptide backbone is the same in the two systems. However, without isotopic labeling of specific peptide bonds we cannot definitely decide whether different parts of the backbone are involved (*31*), although the different band frequencies tend to support this view. It is tempting to assign the positive band at 1617 cm^{-1} to the C═N stretch of the K state. However, a residual band at 1615 cm^{-1} is still present after Schiff base deuteration, which arises from the overlap of this positive band with the large negative band at 1628 cm^{-1} mentioned above. Thus, we rather assign this positive band also to an amide I band, further stressing the different amide I features of the two systems.

The difference band at 1599(+)/1587(−) in the wild-type spectrum completely disappears by the mutation. We assign this band to the asymmetric stretching mode of the negatively charged carboxyl group of the counterion Asp75. This is supported by the observation that this band is essentially still present in the spectrum measured in ^2H_2O (our own data and ref *30*). The shifted frequency in K would indicate the altered interaction of the Schiff base with the Asp75−water 402 complex. In addition, also the region of the symmetric CO_2^- stretching region is influenced by the mutation: we tentatively assign the difference band at 1407(−)/1400(+) cm^{-1} to this mode of Asp75 (the positive part of this band causes the shoulder at this approximate position). However, we cannot exclude contributions from other amino acid side chains.

Time-Resolved Step-Scan FTIR Measurements. The results of the time-resolved step-scan measurements are shown in panels A (amplitude spectra) and B (intermediate spectra) of Figure 3 that were obtained as described in Materials and Methods. As compared to the spectra obtained for the wild-type protein (*12*), the signal to noise ratio is much better in the data presented here. This is due to the considerably shortened photocycle, allowing for much more effective signal averaging. The global fit provides a half-time of 10 ms at 25 °C for the slowest component. This value is in agreement with the time-resolved UV−vis data obtained at 20 °C from which a half-time of 28 ms was deduced (*9*). The data can be fitted with five exponentials. The corresponding intermediate spectra are very similar to each other. It is important to mention that we cannot detect significant differences between the first intermediate spectrum and the spectrum obtained by averaging spectra between 30 and 120 ns (measured with a time resolution of 30 ns; not shown). Thus, we cannot detect relaxation in the nanosecond regime. All of the intermediate spectra are characterized by a positive band at 1526 cm^{-1}, which is assigned to the ethylenic stretch of the retinal. This indicates that all of the intermediates have a similar absorption maximum at 565 nm, in agreement with the UV−vis data. In addition, the typical signature in the fingerprint region (1300−1100 cm^{-1}) shows that in all of the intermediates the chromophore geometry is 13-cis (*12*). Furthermore, the strong HOOP mode between 989 and 997 cm^{-1} already described for the low-temperature K spectrum is also present in all of the time-resolved intermediates. It indicates that they are all characterized by a chromophore that is similarly strongly twisted around the C14−C15 single bond. Thus, the larger twist in the mutant described above is not restricted to the low-temperature intermediate where the protein structure can be assumed to be more rigid. It must be a unique consequence of the mutation influencing in a direct way the environment of the Schiff base. Also, the band pattern in the amide I range (1600−1680 cm^{-1}) is similar in all of the intermediates. This shows that the main distortions of the protein backbone are already present at least within 30 ns and persist with little further changes until the last intermediate. The characteristic difference at 1700(+)/1683(−) cm^{-1} described for the low-temperature spectrum and assigned to the C═O stretch of Asn75 is present in the spectra of all intermediates. Also, this residue is influenced already within 30 ns, and its alteration persists until the initial state is re-formed. As expected from the identification of Asp75 as the proton acceptor for Schiff base deprotonation in the wild type, no protonation of a carboxyl group is observed in the mutant.

The comparison of the first intermediate spectrum and the low-temperature K spectrum (Figure 2b) shows great similarity, taking into account the different spectral resolution (8 vs 4 cm^{-1}, respectively). However, two features cannot be explained by this instrumental difference. In the time-resolved spectrum, one of the larger amide I bands is located at 1659 cm^{-1}, whereas in the low-temperature spectrum it is at 1657 cm^{-1}. Because of the overlap with bands at lower frequencies, the lower resolution of the time-resolved spectra would rather produce an apparent band position at lower frequencies. However, the higher position allows a better separation from the C═N stretch at 1640 cm^{-1}. On the other hand, the amide I band at 1630 cm^{-1} and the C═N stretch are poorly resolved in the time-resolved spectrum, causing an apparent band position at 1638 cm^{-1}. The other difference relates to the ethylenic mode of the photoproducts, i.e., 1532 cm^{-1} (low temperature) vs 1526 cm^{-1} (time resolved). Neither the smaller size nor the altered position of the photoproduct band can be explained by the lower spectral resolution (the bandwidth of the fingerprint bands is not very different from that of the ethylenic modes). Although a clear-cut explanation is not possible at this state, one reason could be that in the time-resolved spectra amide II modes superimpose on the ethylenic bands. Such interference has been described frequently (*12*, *25*, *32*). However, for proof one would have to isotopically label the chromophore. Because

of the differences between wild type and the mutant in the low-temperature K spectra, it is not surprising that also in the time-resolved spectra considerable differences are apparent (see ref *12* for the corresponding spectrum of wild type).

A more careful analysis of the intermediate spectra, however, reveals small but significant changes. This is especially evident from the amplitude spectra. Since the half-times obtained from the global fit differ at least by a factor of 4, the amplitude spectra essentially describe the spectral changes from one intermediate to the next one. In the first two transitions, both chromophore (C15−HOOP mode and fingerprint bands) and protein (amide II at 1543 and 1557 cm^{-1} and several amide I bands) undergo small changes. Generally, the intensity of the HOOP mode decreases continually, indicating a somewhat more relaxed chromophore in the latter intermediates. In the third amplitude spectrum, neither the HOOP mode nor the fingerprint bands of the chromophore can be seen. Only amide I changes and changes between 1530 and 1560 cm^{-1} are present. The latter spectral range is characteristic for amide II bands, but in addition changes of the ethylenic band of the chromophore could also show up. However, since the other bands characteristic of the chromophore are not present, we interpret these features as amide II bands. Thus, this is a transition without changes in the UV−vis, commonly called a spectrally silent transition. In agreement with this, no spectral changes have been detected by time-resolved UV−vis studies (*9*). Such transitions have been described for bacteriorhodopsin (*25*), halorhodopsin (*33*), and the wild-type NpSRII (*12*; see Discussion). It should be emphasized that the small size of the amplitude spectra and, consequently, the great similarity of the intermediate spectra can also be explained by a mixture of states being in a fast equilibrium (*34*), the same species largely dominating in all of the mixtures. In this case, the amplitude spectra would reflect the variations of the small admixtures and, possibly, small depletion of the dominating species. On the basis of our data, however, one cannot decide between the two interpretations of the intermediate spectra. However, in view of the spectrally silent transition, which for the wild-type protein has been correlated with the movement of helix F, we regard, at least for this transition, the latter interpretation of the intermediate spectra as rather unlikely.

Up to the third amplitude spectrum the bands of the dark state do not show up as negative bands. This indicates that up to the fourth intermediate there is no decay to the initial state. However, the fourth amplitude spectrum has already pronounced negative bands of the initial state. These comprise chromophore bands at 1205, 1240, and 1541 cm^{-1}, the Schiff base/amide I bands at 1638 cm^{-1}, the amide I band at 1659 cm^{-1}, and the band due to Asn75 at 1683 cm^{-1}. This excludes a decay to a state with an all-trans chromophore but different protein conformation, such as an O-like state. The partial decay to the initial state causes the smaller amplitudes in the last intermediate. The last two spectra can be explained by a branched photocycle; part of the fourth intermediate (labeled d in Figure 3B) decays directly to the dark state, whereas the remainder passes over an additional intermediate, characterized by the last amplitude spectrum. In this model, the fourth amplitude spectrum describes the transition of intermediate d to the initial state plus its transition to the intermediate on the side path. Therefore, this amplitude spectrum deviates somewhat from the intermediate spectra d and e. As we have discussed previously, under the conditions of kinetic constants differing from each other by more than a factor of 4, not only the shape but also the size of the last amplitude spectrum represents the spectrum of the intermediate on the side path. In addition, intermediate spectrum d in Figure 3B essentially also represents the spectrum of the intermediate at which the branching takes place. It is given by the sum of the last two amplitude spectra (*33*). Under these conditions, we can estimate the percentage of branching to 37%. Since the C15−HOOP mode has a shifted position in the last amplitude spectrum, representing the side path intermediate, one would expect that this shift also shows up in the fourth amplitude spectrum. Indeed, it is located at 990 cm^{-1}, whereas in the intermediate spectrum its position is at 993 cm^{-1}. This difference is indicated in the fourth amplitude spectrum by the presence of a small negative band at 997 cm^{-1} superimposing on the high-frequency slope of the larger positive band. It is important to emphasize that the branching occurring at intermediate d does not influence the evaluation of the earlier intermediate spectra. Although we regard this analysis of the two last kinetic constants as the most plausible, we cannot exclude the possibility that intermediate d decays into a state being in a fast equilibrium with a state very similar to the initial state. However, since the last transition is irreversible, we regard such an equilibrium as rather unlikely.

It is important to mention that although the spectra of the intermediates are very similar, the changes identified by the global fit are reliable. They describe distinct steps during the photoreaction, during which at first chromophore and protein are affected, then only the protein, and finally again chromophore and protein.

DISCUSSION

In contrast to bacteriorhodopsin, where we observed considerable differences between the low-temperature and the nanosecond K intermediates, the two corresponding states of the mutant described here are very similar. They are even more alike than the two respective intermediates of the wild type (*12*). Both UV−vis and FTIR spectra of the wild type showed that the red shift of the absorption maximum of K is very small (10 nm). However, here we described a much larger shift (45 nm). Since in both systems the all-trans → 13-cis isomerization has taken place, it appears interesting to discuss possible molecular causes for the different spectral shifts. One possibility could be the larger distortion of the chromophore described above. Such distortions caused by the not yet relaxed isomerization are generally thought to cause a red shift in the absorption maximum. The red shift from 500 to 530 nm occurring with bathorhodopsin formation, the first photoproduct of the visual pigment rhodopsin, is mainly explained by these distortions, since the environment of the positively charged Schiff base is not altered (*35*, *36*). In bacteriorhodopsin, spectral and structural investigations clearly demonstrate changes in the interaction of the Schiff base with its environment upon formation of low-temperature K (*37*, *38*). In the 1.43 Å K structure, water 402 is still hydrogen-bonded to Asp85, but the isomerization of the chromophore causes a redirection of the NH bond of

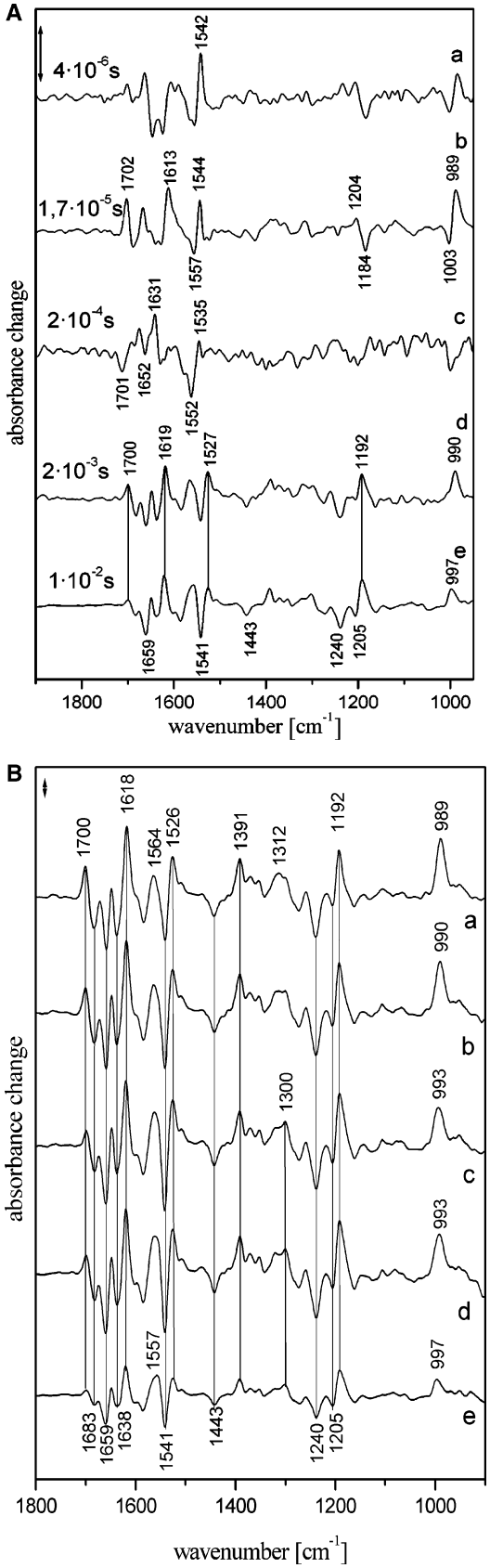

FIGURE 3: Time-resolved spectra of the Asp75Asn mutant. (A) Amplitude spectra obtained by the global fit analysis to a sum of exponentials of the time-resolved step-scan FTIR spectra. The spectra are labeled by their respective half-times. The temperature was 25 °C and the spectral resolution 8 cm^{-1}. The double arrow corresponds to 2 mOD. (B) Intermediate spectra derived from the amplitude spectra presented in (A) using the linear reaction scheme. The double arrow corresponds to 1 mOD.

the protonated Schiff base away from water 402. This induces a weakening of the interaction of the protonated Schiff base with its environment, causing a red shift of the absorption maximum. Since also strong HOOP modes are observed, both chromophore distortion and altered electrostatic interaction will contribute to the red shift of 40 nm, the extent of the respective contributions being difficult to estimate. No structure at comparable resolution is available for low-temperature K of NpSRII. In the published 2.3 Å structure (*39*) water 402 is missing, equally as in the 2.3 Å structure of K of bacteriorhodopsin published by the same group (*40*) and in contrast to the structure obtained at higher resolution. Therefore, this K structure of NpSRII cannot be taken as a reference. However, in view of the higher resolution data of K of bacteriorhodopsin which indicate only little changes of the Schiff base environment, it appears reasonable to assume that also in K of NpSRII the environment is equally little altered. Therefore, the small red shift in K of wild-type NpSR with respect to the dark state could be explained by a still prevailing hydrogen bond of the Schiff base hydrogen with its environment (water 402) and/or by a smaller distortion of the chromophore. Since the HOOP modes have rather small intensity (*12*), the latter mechanism will certainly contribute (*30*). No direct information is available with respect to the former explanation, but a smaller twist of the chromophore would be compatible with a still existing hydrogen bond.

Here it is appropriate to discuss to what extent the band assigned to the 15-HOOP mode indicates distortions responsible for the red-shifted absorption maximum. Our earlier calculations have shown that the HOOP mode gains intensity by twists around neighboring single bonds (*41*). Thus, the intensity of the 15-HOOP mode is an indication of the C14−C15 single bond twist. Large twists (>30°) of this bond would, of course, cause a blue shift, since it interrupts the conjugation. However, this does not apply to smaller twists, which mainly cause a destabilization of the ground state. Our previous calculations have shown that large HOOP intensities are already obtained for twists as low as 15°. In addition, as has been argued for the K structure of bacteriorhodopsin (*38*), a twist of the C=N bond, which will clearly cause a red shift, is counterbalanced by a twist of the neighboring C14−C15 single bond, and larger twists of the former will cause larger twists of the latter. Thus it appears safe to conclude that the intensity of the 15-HOOP mode indicates retinal distortions responsible for a red-shifted absorption maximum.

We now address the large red shift observed for K of the Asp75Asn mutant. Here, the special interaction involving the counterion Asp75, water 402, and the protonated Schiff base is no longer present, causing a red shift of 20 nm of the dark state. The weaker electrostatic interaction in the dark state of the mutant is supported by the smaller deuteration-induced downshift of the Schiff base C=N stretching mode: a larger downshift is taken as an indication of a stronger hydrogen bond (*42*, *43*). Thus, if one assumes similar molecular changes as discussed above for K of the wild type, an even smaller red shift for K of the mutant would have been expected, contrary to what is observed.

Other electrostatic contributions have also to be taken into account: theoretical calculations indicate that, as compared to bacteriorhodopsin, the blue-shifted absorption maximum

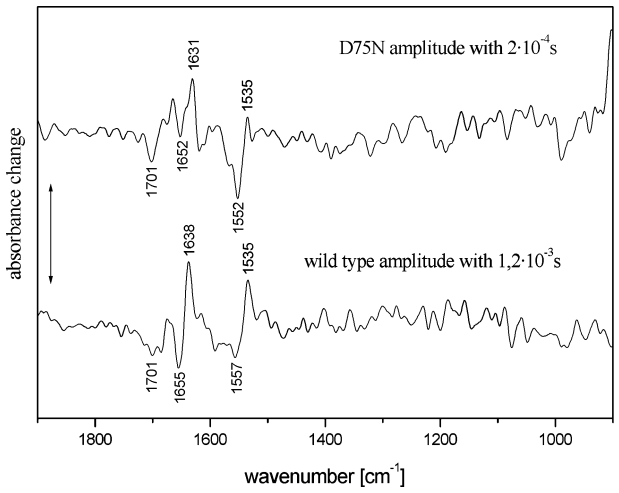

FIGURE 4: Comparison of the time-resolved spectra describing the spectrally silent transition of the wild type (upper trace, reproduced from ref *12*) and of the mutant (lower trace, from Figure 3A). The double arrow corresponds to 2 mOD.

is mainly explained by the outward direction of Arg72, which allows for a more effective interaction of the two negative charges of Asp75 and Asp201 with the protonated Schiff base (*44*), and/or by a smaller distance between the Schiff base and Asp201 on helix G (*44*, *45*). The 20 nm red shift induced by the mutation, considerably smaller than the red shift observed for the corresponding Asp85Asn mutation of bacteriorhodopsin (*46*), indicates that the causes for the blue shift of the absorption maximum are still effective. Although we cannot exclude a major increase of the distance between Asp201 and the Schiff base upon isomerization, in view of the structural data obtained for K of bacteriorhodopsin (*38*), we regard this as less likely. However, it is clear that upon K formation the distance between Arg72 and the carboxylates of Asp75 and Asp201 will not be reduced to an extent that would red shift the absorption maximum.

Thus, it is obvious that a property of the K state so far neglected has to be taken into consideration to explain the large red shift of 45 nm. One clear distinction is the large intensity of the 15-HOOP mode of the mutant K state, indicating larger twists of the chromophore in the Schiff base region. We propose that these larger chromophore twists are the main cause for the considerably larger red shift as compared to the rather small red shift in K of the wild type. Although more retinal proteins would have to be examined to allow for an extrapolation, we suggest on the basis of our FTIR spectra of rhodopsin, bacteriorhodopsin, halorhodopsin, NpsRII wild type, and the mutant investigated here that a large red shift of the early intermediate states is explained by large chromophore twists.

Both the wild type and the mutant have a transition that is spectrally silent in the UV−vis. Figure 4 shows that the corresponding amide band changes are very similar in these two systems, indicating similar backbone changes of the protein. Thus, this transition is not restricted to a state with deprotonated Schiff base. However, it occurs considerably earlier in the mutant (0.2 vs 3 ms at comparable temperatures). This transition is of special interest, since spin label measurements of the wild type indicated a correspondence between this transition and the outward movement of helix F. This movement is thought to be the signal transmitted to the transducer interacting with the receptor via helix−helix contacts (*47*, *48*). Preliminary spin label measurements indicate that such an outward movement of helix F also occurs in this mutant (Steinhoff, Engelhard, et al., unpublished results). It appears that deprotonation of the Schiff base is not a prerequisite for this helix movement. It would be induced by the retinal isomerization but probably requires neutralization of the residue at the counterion position, as discussed in the introduction. Thus, this mutant is expected to show light-induced receptor activation. Indeed, preliminary physiological investigations indicate that *H. salinarum* cells containing this mutant exhibit light-induced repellent response, although the sensitivity of this response has not been determined. In addition, unlike the corresponding mutant Asp73Asn of *H. salinarum* (HsSRII) no constitutive activity has been observed in the mutant investigated here (J. L. Spudich, private communication with respect to both observations). Despite the similarity of the amplitude spectra characterizing the spectrally silent transition of the mutant and wild-type protein, the respective intermediate spectra of the two systems differ considerably, also in the amide I spectral range (*12*). Despite the generally reduced noise in the spectra of the mutant, the noise in the two spectra of Figure 4 is similar. This is due to the shorter time constant of this transition reduced by more than a factor of 10.

The properties of the Asp75Asn mutant can be summarized as follows. In the formation of K at low temperature the reaction has to pass over a barrier, explaining the increase in photoproduct yield with increasing temperatures. This would be in line with the observation that neutralization of Asp85 in bacteriorhodopsin slows down K formation (*20*). The barrier could be caused by altered steric chromophore interactions, leading to a more strongly twisted chromophore. These changes in chromophore protein interaction could explain the decay of K back to the initial state above 180 K. Probably, the movement of helix F is inhibited below this temperature. In contrast, K of the wild-type protein starts to decay above this temperature to M that can be stabilized up to 257 K (ref *49* and our unpublished observation). At 25 °C, the photoreaction passes over several intermediates, all exhibiting a red-shifted absorption maximum. They differ only in small chromophore relaxations and in small protein backbone changes. Especially a spectrally silent transition only involving protein changes is observed, very similar to that the wild-type receptor, although here it is much faster.

How can the faster spectrally silent transition and the faster thermal back-reaction to the initial state be explained? Probably both observations bear on the activation mechanism. The static and time-resolved spectra demonstrate that although light induces the all-trans → 13-cis isomerization, the amide I band changes differ considerably from those observed for the wild-type protein for comparable intermediates or time range. This is probably due to a different protein structure of the dark state. Such a different structure, which even has some properties of the active state, has been inferred from the constitutive activity described for the Asp73Asn mutant of HsSRII (*15*). For the receptor studied here, no constitutive activity has been observed. Nevertheless, it could be that also here the dark state has already some properties of the active state, although not to the same extent as in the HsSRII mutant. A different structure of the dark state is also suggested by the temperature-dependent photoproduct yield,

which is often explained by a barrier in the electronic excited-state potential surface along the reaction coordinate. The wild-type receptor does not show such a temperature dependence. This would indicate that the steric chromophore−protein interaction is altered in the mutant, suggesting an altered structure of the dark state. This altered dark state would be caused by neutralization of the charge at the position of the counterion. A similar conclusion has been reached for the visual pigment rhodopsin (*14*). If this assumption is accepted, it appears feasible that the transition to the signaling state is accelerated. The strong twist of the chromophore, which is, although somewhat reduced, still present in the last two intermediates, could cause the faster back-reaction. Furthermore, it could also be accelerated by the smaller structural changes since the involved barrier will most likely also be smaller.

In comparison to bacteriorhodopsin, the counterion mutant of NpSRII does not exhibit the complex mixture of dark states. The chromophore geometry is only trans, and even at pH 8 no deprotonation of the Schiff base takes place. This indicates that despite the neutralization of the counterion, the dark state is a well-defined entity. Nevertheless, our studies have revealed quite surprising molecular properties of the dark and photoproduct states which bear on the activation mechanism.

ACKNOWLEDGMENT

We thank R. Vogel for critical reading of the manuscript.

REFERENCES

1. Spudich, J. L. (1998) *Mol. Microbiol. 28*, 1051−1058.
2. Tomioka, H., Takahashi, T., Kamo, N., and Kobatake, Y. (1986) *Biochem. Biophys. Res. Commun. 139*, 389−395.
3. Spudich, J. L., Yang, C.-S., Jung, K.-H., and Spudich, E. N. (2000) *Annu. Rev. Cell Dev. Biol. 16*, 365−392.
4. Schäfer, G., Engelhard, M., and Müller, V. (1999) *Microbiol. Mol. Biol. Rev. 63*, 570−620.
5. Luecke, H., Schobert, B., Lanyi, J. K., Spudich, E. N., and Spudich, J. L. (2001) *Science 293*, 1499−1503.
6. Royant, A., Nollert, P., Edman, K., Neutze, R., Landau, E. M., Pebay-Peyroula, E., and Navarro, J. (2001) *Proc. Natl. Acad. Sci. U.S.A. 98*, 10131−10136.
7. Chizhov, I. V., Schmies, G., Seidel, R., Sydor, J. R., Lüttenberg, B., and Engelhard, M. (1998) *Biophys. J. 75*, 999−1009.
8. Kamo, N., Shimono, K., Iwamoto, M., and Sudo, Y. (2001) *Biochemistry (Moscow) 66*, 1580−1587.
9. Schmies, G., Lüttenberg, B., Chizhov, I. V., Engelhard, M., Becker, A., and Bamberg, E. (2000) *Biophys. J. 78*, 967−976.
10. Klare, J. P., Schmies, G., Chizhov, I., Shimono, K., Kamo, N., and Engelhard, M. (2002) *Biophys. J. 82*, 2156−2164.
11. Engelhard, M., Scharf, B., and Siebert, F. (1996) *FEBS Lett. 395*, 195−198.
12. Hein, M., Wegener, A. A., Engelhard, M., and Siebert, F. (2003) *Biophys. J. 84*, 1208−1217.
13. Furutani, Y., Iwamoto, M., Shimono, K., Kamo, N., and Kandori, H. (2002) *Biophys. J. 83*, 3482−3489.
14. Robinson, P. R., Cohen, G. B., Zhukovsky, E. A., and Oprian, D. D. (1992) *Neuron 9*, 719−725.
15. Spudich, E. N., Zhang, W., Alam, M., and Spudich, J. L. (1997) *Proc. Natl. Acad. Sci. U.S.A. 94*, 4960−4965.
16. Spudich, J. L., and Lanyi, J. K. (1996) *Curr. Opin. Cell Biol. 8*, 452−457.
17. Birge, R. R. (1990) *Biochim. Biophys. Acta 1016*, 293−327.
18. Tallent, J. R., Hyde, E. W., Findson, L. A., Fox, G. C., and Birge, R. R. (1992) *J. Am. Chem. Soc. 114*, 1581−1592.
19. Fahmy, K., and Siebert, F. (1990) *Photochem. Photobiol. 51*, 459−464.
20. Logunov, S. L., El-Sayed, M. A., and Lanyi, J. K. (1996) *Biophys. J. 71*, 1545−1553.
21. Gergely, C., Ganea, C., Száraz, S., and Váró, G. (1995) *J. Photochem. Photobiol. B 27*, 27−32.
22. Losi, A., Wegener, A. A., Engelhard, M., Gärtner, W., and Braslavsky, S. E. (1999) *Biophys. J. 77*, 3277−3286.
23. Losi, A., Wegener, A. A., Engelhard, M., Gärtner, W., and Braslavsky, S. E. (2000) *Biophys. J. 78*, 2581−2589.
24. Wegener, A. A., Chizhov, I., Engelhard, M., and Steinhoff, H.-J. (2000) *J. Mol. Biol. 301*, 881−891.
25. Rödig, C., Chizhov, I. V., Weidlich, O., and Siebert, F. (1999) *Biophys. J. 76*, 2687−2701.
26. Ottolenghi, M. (1980) in *Advances in Photochemistry* (Pitts, J. N., Hammond, G. S., Gollnik, K., and Grosjean, D., Eds.) Vol. 12, pp 97−200, Wiley-Interscience, New York.
27. Barth, A. (2000) *Prog. Biophys. Mol. Biol. 74*, 141−173.
28. Gerwert, K., Hess, B., Soppa, J., and Oesterhelt, D. (1989) *Proc. Natl. Acad. Sci. U.S.A. 86*, 4943−4947.
29. Beck, M., Sakmar, T. P., and Siebert, F. (1998) *Biochemistry 37*, 7630−7639.
30. Kandori, H., Shimono, K., Sudo, Y., Iwamoto, M., Shichida, Y., and Kamo, N. (2001) *Biochemistry 40*, 9238−9246.
31. Hauser, K., Engelhard, M., Friedman, N., Sheves, M., and Siebert, F. (2002) *J. Phys. Chem. A 106*, 3553−3559.
32. Fahmy, K., Weidlich, O., Engelhard, M., Tittor, J., Oesterhelt, D., and Siebert, F. (1992) *Photochem. Photobiol. 56*, 1073−1083.
33. Hackmann, C., Guijarro, J., Chizhov, I., Engelhard, M., Rödig, C., and Siebert, F. (2001) *Biophys. J. 81*, 394−406.
34. Chizhov, I. V., Chernavskii, D. S., Engelhard, M., Müller, K.-H., Zubov, B. V., and Hess, B. (1996) *Biophys. J. 71*, 2329−2345.
35. Palings, I., Pardoen, J. A., van den Berg, E. M. M., Winkel, C., Lugtenburg, J., and Mathies, R. A. (1987) *Biochemistry 26*, 2544−2556.
36. Siebert, F., Mäntele, W., and Gerwert, K. (1983) *Eur. J. Biochem. 136*, 119−127.
37. Gerwert, K., and Siebert, F. (1986) *EMBO J. 5*, 805−811.
38. Schobert, B., Cupp-Vickery, J., Hornak, V., Smith, S. O., and Lanyi, J. K. (2002) *J. Mol. Biol. 321*, 715−726.
39. Edman, K., Royant, A., Nollert, P., Maxwell, C. A., Pebay-Peyroula, E., Navarro, J., Neutze, R., and Landau, E. M. (2002) *Structure 10*, 473−482.
40. Edman, K., Nollert, P., Royant, A., Belrhali, H., Pebay-Peyroula, E., Hajdu, J., Neutze, R., and Landau, E. M. (1999) *Nature 401*, 822−826.
41. Fahmy, K., Grossjean, M. F., Siebert, F., and Tavan, P. (1989) *J. Mol. Struct. 214*, 257−288.
42. Baasov, T., Friedman, N., and Sheves, M. (1987) *Biochemistry 26*, 3210−3217.
43. Masuda, S., Torii, H., and Tasumi, M. (1996) *J. Phys. Chem. 100*, 15328−15334.
44. Ren, L., Martin, C. H., Wise, K. J., Gillespie, N. B., Luecke, H., Lanyi, J. K., Spudich, J. L., and Birge, R. R. (2001) *Biochemistry 40*, 13906−13914.
45. Hayashi, S., Tajkhorshid, E., Pebay-Peyroula, E., Royant, A., Landau, E. M., Navarro, J., and Schulten, K. (2001) *J. Phys. Chem. B 105*, 10124−10131.
46. Turner, G. J., Miercke, L. J. W., Thorgeirsson, T. E., Kliger, D. S., Betlach, M. C., and Stroud, R. M. (1993) *Biochemistry 32*, 1332−1337.
47. Zhang, X.-N., Zhu, J., and Spudich, J. L. (1999) *Proc. Natl. Acad. Sci. U.S.A. 96*, 857−862.
48. Krah, M., Marwan, W., Verméglio, A., and Oesterhelt, D. (1994) *EMBO J. 13*, 2150−2155.
49. Hirayama, J., Imamoto, Y., Shichida, Y., Kamo, N., Tomioka, H., and Yoshizawa, T. (1992) *Biochemistry 31*, 2093−2098.

BI0354381